Atmos. Chem. Phys. Discuss., 10, 1221–1259, 2010
www.atmos-chem-phys-discuss.net/10/1221/2010/

Atmospheric Chemistry and Physics Discussions

This discussion paper is/has been under review for the journal Atmospheric Chemistry and Physics (ACP). Please refer to the corresponding final paper in ACP if available.

Testing remote sensing on artificial observations: impact of drizzle and 3-D cloud structure on effective radius retrievals

T. Zinner[1,*], G. Wind[2], S. Platnick[2], and A. S. Ackerman[3]

[1]Deutsches Zentrum für Luft- und Raumfahrt (DLR), Oberpfaffenhofen, Germany
[2]NASA Goddard Space Flight Center, Greenbelt, USA
[3]NASA Goddard Institute for Space Studies, New York, USA
[*]now at: Meteorological Institute, Ludwig-Maximilians-Universität, München, Germany

Received: 9 December 2009 – Accepted: 22 December 2009 – Published: 18 January 2010

Correspondence to: T. Zinner (tobias.zinner@lmu.de)

Published by Copernicus Publications on behalf of the European Geosciences Union.

Abstract

Remote sensing of cloud effective particle size with passive sensors like the Moderate Resolution Imaging Spectroradiometer (MODIS) is an important tool for cloud microphysical studies. As a measure of the radiatively relevant droplet size, effective radius can be retrieved with different combinations of visible through shortwave and midwave infrared channels. In practice, retrieved effective radii from these combinations can be quite different. This difference is perhaps indicative of different penetration depths and path lengths for the spectral reflectances used. In addition, operational liquid water cloud retrievals are based on the assumption of a relatively narrow distribution of droplet sizes; the role of larger precipitation particles in these distributions is neglected. Therefore, possible explanations for the discrepancy in some MODIS spectral size retrievals could include 3-D radiative transport effects, including sub-pixel cloud inhomogeneity, and/or the impact of drizzle formation.

The possible factors of influence are isolated and investigated in detail by the use of simulated cloud scenes and synthetic satellite data: marine boundary layer cloud scenes from large eddy simulations (LES) with detailed microphysics are combined with Monte Carlo radiative transfer calculations that explicitly account for the detailed droplet size distributions as well as 3-D radiative transfer to simulate MODIS observations. The operational MODIS optical thickness and effective radius retrieval algorithm is applied to these and the results are compared to the given LES microphysics.

We investigate two types of marine cloud situations each with and without drizzle from LES simulations: (1) a typical daytime stratocumulus deck at two times in the diurnal cycle and (2) one scene with scattered cumulus. Only small impact of drizzle formation on the retrieved domain average and on the differences between the three effective radius retrievals is noticed for both cloud scene types for different reasons. For the presumably typical overcast stratocumulus scenes, the optical thickness (8 to 9) is large enough to mask the drizzle rain rates at cloud bottom (up to 0.05 mm/h). The cumulus scene does not show much drizzle sensitivity either despite extended drizzle

ACPD

10, 1221–1259, 2010

areas being directly visible from above (locally >1 mm/h), which is mainly due to characteristics of the standard retrieval approach. 3-D effects, on the other hand, produce large discrepancies between the 1.6 and 2.1 µm channel observations compared to 3.7 µm retrievals in the latter case. A general sensitivity of MODIS particle size data to drizzle formation is not corroborated by our results.

1 Introduction

Standard passive cloud optical retrievals are based on simplifying assumptions: (1) clouds are assumed to be plane-parallel homogeneous within each pixel, (2) pixels are radiatively independent, and (3) clouds consist of cloud droplets only, i.e., any drizzle or precipitation modes are ignored. The impact of real cloud situations not fulfilling these assumptions has been investigated in several studies. Cahalan et al. (1994) describe the plane-parallel bias as well as the independent pixel uncertainty caused by the first two assumptions, respectively. Several studies investigated the impacts of both assumptions on standard cloud property retrievals and tried to quantify them (e.g., Loeb et al., 1998; Varnai and Marshak, 2001; Zinner and Mayer, 2006; Varnai and Marshak, 2007). Most were concerned with optical thickness retrievals. Impacts on effective size retrievals have also been investigated (e.g., Platnick, 2000; Chang and Li, 2003; Marshak et al., 2006; Vant-Hull et al., 2007). The third assumption has received much less attention. Minnis et al. (2004) point to the possibility of overestimating effective droplet radius in pristine marine boundary layer clouds containing drizzle, because standard retrievals assume a monomodal, narrow size distribution for cloud droplets. More recently Chen et al. (2008) investigated the detectability of drizzle in the three different MODIS effective size retrievals (using the three different MODIS shortwave and midwave infrared channels). For strong drizzle formation (rain rates >0.1 mm/h at cloud base), the impact on the spectral effective radius retrievals implied decreasing effective radius retrievals with height, instead of the (for boundary layer clouds) usually expected increase with height.

The typical size distribution of cloud droplets used in the radiative transfer simulations that create the forward libraries of plane-parallel cloud properties and reflectances has a relatively narrow fixed width distribution with effective radius as the only free variable. The width of the distribution (effective variance) is usually regarded to be of minor importance. Hansen and Travis (1974) show that the three key single scattering characteristics: the scattering efficiency, the single scattering albedo, and the asymmetry parameter of a size distribution are approaching similar values depending only on its effective radius and hardly on its width in the limit of large particles (large compared to wavelength, i.e., $2\pi r/\lambda \gg 10$). This result is usually adopted for the treatment of radiative transfer in clouds, e.g., in standard retrieval techniques for cloud properties (e.g., Nakajima and King, 1990). For this purpose, Gamma function or log-normal size distributions defined by a range of effective radii (r_{eff}), and by a dimensionless effective variance, v_{eff}, from 0.05 to 0.13 are often used. For example, in the MODIS cloud retrieval MOD06 (Platnick et al., 2003), r_{eff}=4–30 µm and v_{eff}=0.1. From such analytic monomodal narrow droplet size distributions (DSD), optical properties representing non-precipitating water clouds can be derived via Mie calculations.

Once collisional droplet growth becomes active, the size distributions can develop a significant tail. Usually the presence of a few large precipitation size drops is regarded as negligible in radiative transport simulation, because they do not contribute much to the overall cross section that defines the extinction. For rain drops at sizes of much more than 1 mm this is probably correct, but precipitation often develops through a pronounced drizzle stage – especially in a marine boundary layer environment with potentially low cloud condensation nuclei numbers and weak vertical development. Drizzle drops in the size range just beyond typical cloud droplet sizes of 5–15 µm are much more numerous than larger rain drops. This is why some studies suspect or show that drizzle formation is detectable in passive remote sensing observations (Chang and Li, 2003; Minnis et al., 2004; Chen et al., 2008; Leon et al., 2008; Lebsock et al., 2008).

At the same time, MODIS observations of low marine cloud horizontal morphology, which is often associated with drizzle processes, can show interesting microphysical features. Figure 1 shows a false color composite image of open and closed marine stratocumulus cells in the subtropical Atlantic (∼28° N, 60° W). Obvious is the difference in coloration of the open cells, usually linked to drizzle formation (Stevens et al., 2005; Wood et al., 2008), seen in the upper left/middle portion of the image, compared to the closed cells just to the south (left central part of the image). In this false color image, red hues mark cloud regions with reduced shortwave infrared (SWIR) reflectances compared to the visible and near-infrared parts of the spectrum. This smaller ratio can result from large, strongly absorbing ice particles (cf. the cirrus clouds in the lower right) or from large droplets. The evaluation of the MODIS effective radius retrievals for the open cell area in the upper left of Fig. 1 reveals that the r_{eff} retrievals from the 0.86/3.7 µm channel combination shows smaller droplets than the retrieval from 0.86/2.1 µm combination (Fig. 2).

This would be consistent with the picture that for the channel where radiation is less absorbed by liquid water, 2.1 µm, the increasing influence of drizzle formation deeper down in the cloud is detectable while the 3.7 µm signal, where liquid water is strongly absorbing, is only affected by the particles from a shallower layer at the top of the clouds where drizzle modes are not significant.

Other candidate sources for this type of difference are shadow effects or cloud masking deficiencies affecting the MODIS retrieval. Cloud top height variations are large in this cloud type and region causing sharp shadows; cloud masking is not easy in this type of cloud with strong small scale contrasts of illuminated, shadowed, and cloud free areas. Both effects have the potential of mimicking large effective radius retrievals (Marshak et al., 2006). However, in Fig. 1, shadowing would be expected to preferentially cause a high r_{eff} bias when looking toward the sun (right side of image for this MODIS Terra case), which is not evident. Regardless, 3-D effects would be expected to be stronger for weaker absorbing channels (1.6 or 2.1 µm) relative to 3.7 µm, which would give the opposite difference between the retrievals from that seen in Fig. 2.

There is no direct, unambiguous way to separate the various effects and therefore no simple way to validate any of the conclusions one might reach by analyzing the satellite observations alone. The large majority of investigations in the field are carried out on a theoretical level, e.g., generalized or simplified cloud structures used for forward radiative transfer simulations with little concern for specific realism of cloud structures, cloud microphysics, or retrieval algorithms. Alternatively, investigations are based on observational evidence alone, mostly satellite data without full knowledge of the underlying "truth", or available ground truth data, with very limited spatial coverage. Another approach is to use of synthetic satellite data based on realistic cloud simulations. Retrievals can be applied to these synthetic observations and subsequently retrieved properties can be compared to the given cloud properties. This approach has the further advantage that radiative transport (1-D or 3-D) as well as cloud condition (e.g., with or without drizzle, diurnal evolution, etc.) can be modified in a targeted manner to test the sensitivity of retrievals to the modified characteristic. The retrieval results can be analyzed within a fully controlled testing environment.

The cloud microphysical data sets for our tests are simulated with a Large Eddy Simulation (LES) cloud resolving model with size-resolved microphysics (Sect. 2). These marine boundary layer realizations are pre-processed to reduce the complexity of the full 3-D size distributions, in order to serve as input to a radiative transfer simulation and in order to separate a drizzle from the cloud droplet mode in the simulated size distributions (Sect. 3). The associated optical properties are discussed in Sect. 4.1. Section 4.3 presents the application of the MODIS-like cloud property retrieval for the derivation of effective radius from the simulation of 5 spectral channels (Sect. 4.2). Section 5 discusses the outcome of the sensitivity studies.

2 Cloud model

For the cloud model we use a 3-D large-eddy simulation code that resolves the size distributions of aerosol particles and liquid water drops (Ackerman et al., 2003). We analyze the results from two simulations: (1) an overcast stratocumulus case based on an idealization of conditions observed during the FIRE-I field project (a case described by Ackerman et al., 2004), and (2) a trade cumulus case based on a idealization of conditions observed during the RICO campaign (described in an unpublished manuscript by Margreet van Zanten and co-authors). Table 1 gives an overview of the model setup for the simulations used in the following. Figure 3 shows some features of the stratocumulus deck at two times in the simulation (Sc 2 p.m. and Sc 6 p.m.).

For the stratocumulus simulations, the model uses 25 size bins with droplet radius mid-points up to 256 µm. The grid mesh is 64×64×64, with uniform 52.5-m horizontal grid spacing and a stretched vertical grid that has minimum spacing of ~5 m at the surface and at the initial cloud-top height. A total particle concentration (initially all particles are unactivated condensation nuclei) of 40 cm^{-3} is used; the domain-averaged droplet concentration (weighted by cloud water mixing ratio) is about 30 cm^{-3}, thus these simulations represent very pristine conditions. Solar radiation is included in the simulations, for a date of 14 July at a latitude of 33° N, and the simulation starts at 6 a.m., shortly after sunrise. The simulations produce an overcast marine stratocumulus deck. Over the 12-h period, the simulations show slightly decreasing cloud heights (top and base), increasing optical thickness, and increasing precipitation rate. The model output used here are for two time slices, at 2 and 6 p.m. 2 p.m. matches a typical MODIS overpass time while the 6 p.m. scene is a slightly different scene, with larger domain-average precipitation rate at cloud base (0.02 and 0.05 mm/h at 2 and 6 p.m.) and optical thickness (7.8 and 9.4 at 2 and 6 p.m.). The optical thickness at the two output times is in the range typically observed for marine stratus by MODIS (Platnick et al., 2003), while the effective radius at cloud top is between 15 and 20 µm, at the upper end of the expected range, consistent with droplet concentrations being lower than those typically measured.

For the trade cumulus simulation, the model uses 25 broader size bins that span droplet radii mid-points from 1 to 1100 µm. In this case the grid mesh is 128×128×100, with uniform horizontal and vertical grid spacing of 100 and 40 m, respectively. The cloud-free aerosol distribution is bimodal with total concentration 105 cm^{-3}, with 15 cm^{-3} of those in the coarse mode (representing sea salt). The treatment of radiation

ACPD
10, 1221–1259, 2010

is extremely simple, with only an imposed, fixed profile that represents clear-sky cooling only. The 24-h simulation produces a field of broken cumulus clouds with average real coverage of about 20% and an average droplet concentration (weighted by cloud water mixing ratio) varying between 50 and 60 cm^{-3}. Temporal and spatial variation of precipitation is substantial, with cloud-base domain averages reaching values of 0.02 mm/h and greater, while local peaks are two orders of magnitude greater.

Figure 4 shows drop size distributions from one of the cases. All the selected distributions have an effective radius of 15 µm. The standard assumption for passive cloud property retrievals is a narrow DSD without considering potential drizzle. Such a distribution is represented by the broken black line in Fig. 4, a Gamma distribution with v_{eff}=0.05. All other lines show randomly selected distributions from the cloud data. It is obvious that distributions in this drizzling case are generally wider than the assumed Gamma DSD. Only the narrowest distributions are similar to the standard Gamma distributions.

3 Separation of cloud and drizzle modes

The reason for the use of narrow analytic functions (e.g. Gamma with fixed variance) for the derivation of cloud optical properties for radiative transfer simulations is to cover a realistic range of (non-drizzling) drop size distributions by modifying a single parameter – the effective radius. Likewise, the retrieval only has to estimate a single microphysical parameter regarding the size distribution. Thus, forward and backward radiative transfer solutions do not have to consider the full variety of realistic size distributions (Fig. 4), but can use a table of optical properties as a function of effective radius. Once the size distribution is broadened due to precipitation, the table of optical properties and forward radiative transfer tables has to include at least one additional dimension – the width of DSD. For the backward radiative transfer problem – the retrieval – this would in turn increase the number of retrieval unknowns, most likely exceeding the information content in observations from a few spectral channels.

At least the width of the distribution has to be considered as a second variable on which the optical properties in a radiative transfer model depend. We decided to simplify the variety of real drop size distributions from the cloud model for the radiative transfer simulation of synthetic MODIS observations by specifying a narrow cloud droplet mode separate from a wider drizzle mode. With such a bimodal fit, we are able to approximate size distributions like the ones shown in Fig. 4.

Figure 5 shows two examples of this approximation. Two Gamma functions – one representing the cloud mode and one representing the drizzle mode – are fitted (minimizing the cross sectional deviation) to each distribution from the cloud model. In a first fit r_{eff1}, r_{eff2}, as well as v_{eff1}, and v_{eff2} of the Gamma functions are free parameters. Parameters r_{eff1} and v_{eff1} belong to the small droplet cloud part of the original DSD, r_{eff2} and v_{eff2} to the drizzle drop mode. These parts are defined as either the droplets left and right of a local minimum in the DSD (two separate modes) or the droplets smaller and larger than twice the effective radius of the complete distribution. A fit is first found for the cloud mode and successively for the remaining drizzle mode (including the remaining part of the small droplets). To reduce the number of variables for the following radiative transfer simulations, the optimal values for the width of both functions are fixed to the mean values of all distributions in the 3-D field of v_{eff1} and v_{eff2}. Thus for the second fit, the widths are fixed to 0.1 and 0.175, respectively. In this way, the whole variety of simulated DSD from the model is reduced to an analytic representation: two sets of Gamma functions depending only on r_{eff1} and r_{eff2}. In the first example shown in Fig. 5 (left panel), a well-defined bimodal DSD with r_{eff}=15 µm is approximated by a cloud effective radius of 8.5 µm and a drizzle effective radius of 52.5 µm; a second example (right panel) with the same r_{eff} has no prominent second mode and is approximated by a larger r_{eff1}=14 µm and a smaller r_{eff2}=43 µm. Most distributions in Fig. 4 are approximated well in this way.

The decomposition of the DSD allows more efficient Mie calculations of scattering properties for the distributions. For the two sets of Gamma functions, optical properties are pre-calculated to form two traditional look-up tables (properties as function of r_{eff})

to be used in the radiative transfer calculations. To specify the extinction in the two modes, the water content is divided into cloud water and the drizzle water for each LES cloud model grid box (conserving the total LWC). Thus two 3-D fields associated with each mode, having separate water contents and effective radii, are combined from the look-up tables to give the optical properties for a drizzling cloud scene.

The resulting field of cloud and drizzle water fields for the right hand column of panels in Fig. 3 are shown in Fig. 6. The spatial separation of the two droplet modes is obvious. Precipitation water (drizzle mode, right column of Fig. 6) below the cloud base around 200 m extends below the cloud deck (cloud mode, left column). The continuity of the fields of drizzle water content and drizzle effective radius in and outside the cloud layer also seems to corroborate the capability of the separate fits. The effective radius in the cloud mode is still rather large (average of 17 µm); in the drizzle mode values are much larger (average of 60 µm). A few regions show very large "cloud mode" droplets with values around 40 µm below the cloud deck (at 0 to 150 m). These regions are dominated by the precipitating drops from the cloud deck above, leading to a stronger single large precipitation mode in the size distribution. If this single mode is found at relatively small droplet sizes, it is misinterpreted as being in the cloud mode. Apart from these minor issues, the separation of small cloud droplets and large drizzle drops is physically plausible in this scene, and regardless, provides an efficient mechanism for determining optical properties as discussed in the next section.

4 Results

4.1 Optical properties of drop size distributions

Figure 7 shows optical properties for size distributions from the stratocumulus cases. 50 sample distributions were randomly selected for each of the following effective radii: 6, 8, 10, 12, 17, 20, 25, and 30 µm. Three calculations of Mie properties were conducted for each distribution: (1) using the original size distribution from the cloud model, (2) assuming the classical narrow single mode Gamma distribution with the

ACPD
10, 1221–1259, 2010

same effective radius and v_{eff}=0.1, and (3) using the fitted bimodal Gamma size distributions presented in Sect. 3. In Fig. 7, mean values over the 50 samples are shown for each of the three calculations for four MODIS channels. In channels dominated by scattering the properties, the actual size distribution (black lines) can be well approximated by the properties of the narrow standard Gamma distribution (red lines). Only for the asymmetry parameter do noticeable deviations appear. The stronger the absorption ($1-\varpi_0>0$), the larger the deviations become. In MODIS channel 20 (2.1 µm), not only are the asymmetry parameters of the narrow size distributions clearly different from the actual wide size distributions with the same effective radius, but same is true of the single scattering albedo. While these deviations in ϖ_0 might appear small, they are equivalent to single particle absorptivity differences of 10% and more.

The possibility of describing single scattering properties of realistic wide (drizzling) size distributions using the narrow single mode Gamma distributions obviously varies with wavelength. The differences in optical properties in our cases are not as large as the ones demonstrated in Minnis et al. (2004). But while Minnis et al. (2004) investigated theoretical size distributions (loosely based on observations) and speculated on possible drizzle impact, our results are based on a number of realistic size distributions from a physical model simulating drizzle formation.

At this point it is interesting to check the potential of these differences in optical properties to affect the retrieveable effective radius, neglecting any realistic cloud structure or full radiative transfer. A first estimate is found by applying the optical properties from Fig. 7 in a radiative transfer experiment for a plane-parallel single layer cloud. This way, two different radiance solutions can be obtained from the optical properties for the idealized Gamma size distribution and the average of the real sample distributions of the same effective radius. The successive application of the retrieval results in relative deviations in effective radius between 13% (using 1.6 µm) and 17% (3.7 µm). Accordingly, the differences in size distribution, and thus optical properties, in principal have the potential to cause the observed deviations in effective radius of several micrometers between MODIS retrievals using channel 6 or 7 and the ones using channel 20.

ACPD

10, 1221–1259, 2010

The question how such errors in the single particle properties affect the full radiation field of a cloud structure with varying density and a mixture of particle sizes, has to be answered by more complete simulations in the next section. Apart from that, Fig. 7 shows that the bimodal fit to the real drop distributions is an excellent approximation with respect to the representation of their single scattering properties (green dot-dashed lines).

4.2 Radiative transfer simulations

The radiative transfer is simulated using the libRadtran package (Mayer and Kylling, 2005). For the simulation of synthetic MODIS observations, the 3-D Monte Carlo solver MYSTIC is used (Mayer, 2000). MYSTIC accepts two 3-D fields of cloud properties and related optical properties tables (usually used to provide ice and water cloud input). This feature is used to set up the separate cloud and drizzle 3-D fields. Optical properties are calculated as a function of effective radius for the narrow cloud droplet mode (Gamma distribution with v_{eff1}=0.1) and the wide drizzle drop mode (v_{eff2}=0.175) using a Mie code. Band models of MODIS channels 2, 6, 7, 20 and 31 (10.8 µm) are used to simulate the radiance at top of atmosphere for a nadir view and solar zenith angle of 45°. To limit the number of possible effects on the retrieval algorithm to a minimum, influences by other atmospheric constituents and the surface are neglected (albedo=0, emissivity=1).

Four different simulations of satellite reflectance are conducted for each of the three LES data sets given in Table 2 with the aim of separating the different effects for analysis: a full 3-D simulation with and without the drizzle field, and a 1-D independent column simulation that excludes horizontal transport effects (again with and without the drizzle). Examples of the simulations are shown in Fig. 8. The simulation is done on the full cloud model resolution (52.5 m or 100 m) and the results are then averaged to 500 m spatial resolution. On the usual MODIS cloud product resolution of 1 km only very few pixels could be obtained, for this reason the following analysis is done on this slightly higher resolution.

In the near-infrared channels (i.e., channel 2, Fig. 8b and c) the optically thicker portions, and especially the illuminated cloud slopes, show high reflectance. Similarly (and thus not shown) for channels 6 and 7. Channel 20 shows the sum of separate solar reflectance and thermal emission contributions (Fig. 8e and f). Due to the almost constant cloud top height, and thus constant thermal background, the simulated channel 20 appears much more homogeneous. The lowest radiances in Fig. 8e are for shadows close to the very thin cloud portion. This is generally the same region where the thermal surface contribution leads to the largest net emitted radiance (surface temperature 288 K, cloud-top temperature 285.5 K). For all cloud scenes 500 m results are generated for the cloud droplet fraction with and without the precipitation fraction. In addition, independent column simulations of the same cases are provided. This way, 3-D radiative effects due to cross pixel horizontal transport like shadows and bright slopes can be excluded.

4.3 Particle size retrieval

All operational retrievals use the different sensitivities to cloud optical thickness and droplet effective radius at predominantly scattering wavelengths in the visible/near-infrared and more absorbing near shortwave/midwave-infrared wavelengths, respectively (e.g., MODIS, Platnick et al., 2003). In the MODIS algorithm (generically referred to by the MODIS Terra product name, MOD06) several independent retrievals of effective radius are done using different combinations of the visible/near-infrared and/or channels 6, 7, and 20 (where liquid water absorption becomes progressively important).

Instead of using the available plane-parallel homogenous (PPH) cloud model vs. radiance libraries in the MODIS MOD06 algorithm, the libraries were re-generated using the libRadtran package according to the above mentioned settings to eliminate spurious effects due to radiative transfer model inconsistencies. The libraries were generated by the libRadtran package also for the reason that the radiative transfer

ACPD
10, 1221–1259, 2010

code used to create the operational MODIS libraries does not provide cloud emissivity, necessary for proper emission correction of the measured 3.7 µm radiance. The measured radiance in the 3.7 µm channel includes a significant emissive component, which is a combination of transmitted thermal emission from the surface and from the cloud (both of which depend on cloud optical thickness and effective radius). In order to properly estimate the amount of emission, the cloud top temperature and pressure (for atmospheric correction) is required. For the stratocumulus clouds under study, such retrievals are obtained from the MODIS 11 µm window (Menzel et al., 2008). A side effect that the complication of obtaining asymptotic theory parameters (King, 1987) that are used in the original MOD06 libraries is also reduced this way.

The retrieval of optical thickness and effective radius is explained elsewhere (Nakajima and King, 1990). As with MOD06, three separate size retrievals are performed using simulations of the MODIS 0.86 µm channel along with the 1.6 µm, 2.1 µm or 3.7 µm channel simulations. The operational MOD06 algorithm interpolates across the library geometry space for the given solar and sensor zenith angles and the relative azimuth. In this study, however, the libraries were custom generated to match the model geometry and no interpolation is therefore needed.

4.3.1 Base case: overcast stratocumulus

Figure 9 shows the results of the retrievals applied to the 3-D simulated MODIS observation for the 2 p.m. stratocumulus case. The retrievals can be compared to the original LES cloud data sets (Fig. 8a and d). Because effective radius in real clouds usually varies with height, and each of the MODIS retrievals has a certain penetration depth into the cloud layer, an estimate for the "true" retrieved size is required. It has been shown that the expected size is approximated by a reflectance weighting that is a function of the size profile, geometry, and spectral band (Platnick, 2000). Rather then replicate the spectral reflectance weightings across the model field, we have opted to instead use an easier extinction weighting (down to a maximum optical depth of 5,

ACPD
10, 1221–1259, 2010

Title Page
Abstract Introduction
Conclusions References
Tables Figures
◀◀ ▶▶
◀ ▶
Back Close
Full Screen / Esc
Printer-friendly Version
Interactive Discussion

cloud top layer effective radius, Fig. 8d). However, the more relevant point is not the determination of these reference values, but the differences between the three spectral retrievals.

The high resolution retrievals (MOD06 run on the full 50 m resolution, Fig. 9a–c) show a slight shift of the maximum optical thickness towards the sun. The average retrieved optical thickness slightly overestimates the true value for the 1-D as well as the 3-D simulated observation. The effective radius retrievals show much stronger sensitivity for illumination effects. In shadowed areas the effective size is strongly overestimated while it is underestimated for the illuminated parts. Using 1.6 µm no retrievals are found for some of these areas (additional white pixels). This is due to ambiguities appearing in the assignment of effective radius and optical thickness in the PPH retrieval libraries. Figure 9d–f shows the retrievals for the same case using simulated radiances at 500 m resolution. 3-D effects which are generally small for these cases, widely disappear due to the averaging over large pixels.

The following analysis combines the 500 m results for both overcast simulations; a sample of 72 overcast stratocumulus pixels is examined. Tables 2 and 3 show average retrievals and related standard deviations. Only very small 3-D impact can be seen. Comparing 1-D and 3-D simulations the average values change only between −0.15 (for retrieval 0.86/1.6 µm) to 0.16 µm (retrieval 0.86/3.7 µm), and even the standard deviation shows only a small increase in scatter. The mean retrieved values also hardly change due to drizzle either (between 0.1 to 0.3 µm increase in r_{eff} with drizzle). Still there are some interesting details to be noted.

The cloud deck in both cases has a consistent vertical profile as far as the cloud droplet mode is concerned; droplet effective radii are increasing with height (Fig. 6). Thus retrievals having a deeper optical penetration depth show smaller average effective radii characteristic of droplets at lower altitudes. The "true" values averaged over the cloud top layer give a reasonable match to the 0.8/2.1 µm retrieval. While the retrieval using 3.7 µm especially for the 1-D simulations shows very good 1:1 matches to our "true" values for a wide range of retrievals (not shown), the mean is slightly larger.

ACPD
10, 1221–1259, 2010

Drizzle and 3-D structure impact on effective size retrievals

T. Zinner et al.

The retrievals using 1.6 µm are a bit smaller because they are more sensitive to effective radius in lower cloud layers. These differences demonstrate the potential to retrieve information on the cloud profile from the different spectral retrievals (e.g., Chang and Li, 2003; Chen et al., 2008). The scatter in the 1-D no-drizzle case is smallest for the 3.7 µm retrieval due to its having the smallest inhomogeneities of particle size near cloud top within the 500 m pixel. This plane-parallel error is caused by the non-linear relation between radiance and the retrieved property (especially optical thickness). As the MODIS retrieval simultaneously retrieves optical thickness and effective radius for each pixel (from two channels) the solutions and errors of each single retrieved parameter always affect the other parameter as well. An advantage of the retrieval using 3.7 µm is the better orthogonality of the two solutions, and so the retrieved effective radius is nearly independent from the optical thickness (e.g., Platnick et al., 2001). This independence from plane-parallel biases in the optical thickness retrieval (at least in the investigated range of optical thicknesses) leads to less variability in the 3.7 µm 1-D retrieval. There is however a greater uncertainty in the retrieval of 3.7 µm cloud effective radius due to uncertainty in the amount of emission present in the signal.

Moving on to the 3-D results, the scatter increases due to horizontal photon transport (shadows, bright slopes) though the effect is relatively benign. Interestingly the relative increase in scatter is greatest for the 3.7 µm retrieval. Due to greater absorption the horizontal photon transport is much weaker in this channel compared to 1.6 and 2.1 µm. The greater absorption causes sharper shadow effects and thereby stronger 3-D impact on the scatter. Mean values over all pixels are practically unchanged.

Adding the drizzle mode to the cloud data set has only minor impact. A slight increase of the retrievals using 1.6 and 2.1 µm is detectable in the average values as well as in the individual retrievals while even smaller sensitivity is seen for the 3.7 µm retrievals. Drizzle mainly forming in the central and lower height levels of the cloud is only detectable in the deeper penetrating retrievals while the retrieval that sees the topmost cloud layers changes least. The overall impact is minimal (0.3 µm on average) and hardly large enough to make drizzle formation directly detectable from effective

ACPD
10, 1221–1259, 2010

radius retrievals in this case. Chen et al. (2008) show that for heavy drizzle, the impact can lead to a reversal of the usually positive droplet size gradient with height (consistent with increasing size retrievals with increasing wavelength) towards a neutral or negative size gradient with height (as apparently seen in Fig. 2) though their study involved analytic ad hoc size profiles and were not developed from model fields or in situ data.

There is obviously little drizzle sensitivity in this case. The cloud is thick enough to obscure the drizzling lower cloud layers and the drizzle rain rate is at the same time rather small (0.02 and 0.05 mm/h average at cloud base in the two scenes) compared to reported cases where drizzle formation seems to have impact on MODIS retrievals (>0.1 mm/h in Chen et al., 2008).

4.3.2 Complex case: scattered cumulus

Beyond the just discussed base case, an overcast stratocumulus deck with a typical marine diurnal cycle that does not show sensitivity of cloud retrievals to drizzle, we now investigate a second case with heavier precipitation and greater horizontal heterogeneity. In the broken cumulus case introduced in Sect. 2, localized heavy drizzle, with peak precipitation exceeding 1 mm/h in some model columns is in some places directly visible from the simulated satellite perspective, as the precipitation shears from its generating cells, which in some instances have largely dissipated. Figure 10 shows the 2-D fields of optical thickness and cloud top layer effective radius from the LES as well as the 3-D simulated high resolution nadir radiance field for the 2.1 µm channel. The fields of drizzle and dissipating clouds show up as dark red areas in Fig. 10b (effective radius ≫30 µm). As before simulated MODIS observations at 500 m resolution are processed through the MOD06 retrievals. Figure 11 shows these retrievals of optical thickness and effective radius using 0.86/2.1 µm and 0.86/3.7 µm, Tables 4 and 5 show the domain average values and their standard deviation.

In this scattered cumulus case an important additional factor is the number of pixel retrievals possible. If the reflected signal in one of the channels is not part of the PPH cloud model vs. radiance libraries (e.g. the signal is too low) or the combination of two channel's reflectivities is outside the covered retrieval space a non-retrieval is issued. In addition, an unambiguous is not possible for all of these cloudy pixels. This problem already shows up in the optical thickness retrieval, as seen in Table 4. The retrieval substantially underestimates the domain average even for the 1-D simulated observations. Partly the underestimation is due to the plane-parallel bias (averaging over inhomogeneities leads to underestimation), but partly also to areas of small optical thickness (e.g. in the drizzle areas) for which no retrievals are found on the 500 m resolution. This effect manifests itself also in the standard deviation which is much larger for the LES optical thickness field than for the retrieved fields due to the missing small values in the latter. Moving to full 3-D simulated MODIS data the underestimation of the real optical thickness increases. 3-D illumination effects and diffusion of radiation away from the cloud patches obviously reduces the reflected radiance and thus the retrieved optical thickness.

In contrast to the overcast stratocumulus case, the LES domain averages of the cloud top layer effective radius are dominated by the presence of drizzle. The domain average is larger than 50 µm including the drizzle mode while it is only about 20 µm without. This difference is evident in any of the retrievals, as no retrievals are possible for the large areas with drizzle but no cloud water content at cloud top, because they are too dark to be considered cloud. Only a minor increase of droplet size of about 0.5 to 1 µm is found by the 3.7 µm retrieval once the drizzle is included (for 1-D and 3-D MODIS simulations). Also the impact of 3-D radiative transfer is hardly detectable, both for the averages and the standard deviations. The 3-D impact is different for the 1.6 and 2.1 µm retrievals. The domain average retrieved sizes in some cases even decrease, when drizzle is added. This apparently contradictory result is a consequence of a few additional, but small, retrievals. These retrievals appear in regions close to the cloud edges where especially large retrieved sizes are visible in the 3.7 µm data (compare Fig. 11b and c). These locations indicate optically thin layers of large drops (visible in the most absorbing channel) covering a layer of much smaller cloud droplets (detected by the more penetrative channels). Alternatively, the size of these small values is at

ACPD
10, 1221–1259, 2010

the low end of the effective radius range covered by the MOD06 retrieval libraries, and thus the different 3-D response of the retrieval at 3.7 µm could also be an artifact of misinterpretations of the "observed" radiance at he limits of the lookup-up tables. If only the pixels are considered which produce retrievals for all three channels, the different 3-D response of the retrievals at 3.7 µm disappears and the average effective radius increases for all three (not shown).

The impact of 3-D effects is only obvious for the 1.6 and 2.1 µm retrievals. The retrieved effective radius is reduced by several micrometers for both (Table 4). This reduction could be due to cloud slopes illuminated by the sun then misinterpreted as small particles while for the related shadow regions no retrievals are derived at all (compare Figs. 10c and 11b), but again the number of spurious small retrievals increases for the 3-D simulated MODIS observations compared to the 1-D simulations and reduces the domain average additionally.

5 Discussion and outlook

Results of a model study on the sensitivity of the MODIS operational cloud effective radius retrievals to the presence of drizzle and 3-D radiative transfer are presented. This study is done using LES cloud data sets with detailed microphysics, through the simulation of synthetic MODIS images with a Monte Carlo model, and the successive application of the MODIS retrieval to the simulated observations. The droplet size distributions from LES are separated into precipitation and cloud droplet modes. In this way, the prerequisite Mie scattering calculations needed for the radiative transfer simulations are provided via two look up tables that are a function of effective radii with fixed (though different) effective variances. Realistic optical properties for a wide range of droplet size distributions are shown to be represented by a combination of the two look up tables. Impacts of drizzle and 3-D radiative transfer are thus investigated separately by systematic modification of certain parts of the simulated testing environment (drizzle or no drizzle, 1-D or 3-D radiative transfer).

ACPD

10, 1221–1259, 2010

Drizzle and 3-D structure impact on effective size retrievals

T. Zinner et al.

We investigate two different types of boundary layer clouds: (1) a case of a drizzling fully overcast marine stratocumulus deck at two stages during a diurnal cycle; and (2) a more complex cloud scene of a drizzling cumulus field. For both cloud types the impact of drizzle formation on the MODIS retrieval is very small. The sensitivity to the drizzle size drops in the cloud deck is too small to explain contrast like that seen in Fig. 1 let alone a clear detection of drizzle. The lack of substantial cloud gaps (i.e., the overcast nature of the scene) prevents a direct view of drizzle below the cloud layers for the stratocumulus case while in the cumulus case the large areas of theoretically openly visible drizzle remains undetected as the reflectance from these regions is too low to produce a retrieval. The effect of 3-D radiative transfer is only pronounced for the scattered cumulus case and the size retrievals using channels 6 and 7 (1.6 and 2.1 µm).

The analysis of the cumulus case suggests some additional sources of difference between the different MOD06 effective size retrievals. Non-retrievals, which are more likely the shorter the wavelength of the absorbing channel and the weaker the absorption is, can have a significant impact on domain averages. This effect can be increased by 3-D effects through the different sensitivity to shadowing and illumination for the three retrievals. In addition, most likely spurious small pixel retrievals in situations close to ambiguous solutions in the retrieval space further contribute to a lack of retrievals.

Drizzle formation as well as 3-D effects in clouds with larger scale dynamical organization, like the cell structures in Fig. 1, can probably produce larger horizontally averaged rain rates than the 0.02 and 0.05 mm/h in the stratocumulus simulations used (local peaks exceed 0.2 and 1 mm/h for the stratocumulus and cumulus scenes here) or 3-D effects which have, depending on the illumination geometry, different impact. In this respect, this work has to be seen as a first step. We exclude the possibility that the MODIS effective size retrievals are affected neither by the non-representation of wide (drizzling) droplet distribution in the retrieval itself nor by un-identified uncertainties in the emission correction of the solar/terrestrial channel 20 (3.7 µm) at least for the cloud scenes we consider. In addition, we see no sign that presumably typical daytime

ACPD
10, 1221–1259, 2010

Drizzle and 3-D structure impact on effective size retrievals

T. Zinner et al.

drizzle for very clean daytime marine stratocumulus can be detected in MODIS products. Even for the broken cloud scene we consider, no strong sensitivity of the MODIS retrieval to drizzle is found. 3-D effects, on the other hand, show the potential to introduce large discrepancies in retrieved effective radius between the three different retrievals; although in the case we examine these have a different effect than for the case presented in Figs. 1 and 2. The application of our testing setup to more organized cloud situations is left for further study.

Acknowledgements. T. Zinner was supported by a German Research Foundation (DFG) Fellowship and the NASA visiting scientists program. We thank M. Hagen for his helpful comments on the manuscript.

References

Ackerman, A. S., Kirkpatrick, M. P., Stevens, D. E., and Toown, O. B.: The impact of humidity above stratiform clouds on indirect aerosol climate forcing, Nature, 432, 1014–1017, doi:10.1038/nature03174, 2004.

Ackerman, A. S., Toon, O. B., Stevens, D. E., and Coakley, Jr., J. A.: Enhancement of cloud cover and suppression of nocturnal drizzle in stratocumulus polluted by haze, Geophys. Res. Lett., 30, 1381, doi:10.1029/2002GL016634, 2003.

Cahalan, R. F., Ridgway, W., Wiscombe, W. J., Gollmer, S., and Harshvardhan: Independent pixel and Monte Carlo estimates of stratocumulus albedo, J. Atmos. Sci., 51, 3776–3790, 1994.

Chang, F.-L. and Li, Z.: Retrieving vertical profiles of water-cloud droplet effective radius: Algorithm modification and preliminary application, J. Geophys. Res., 108(D24), 4763, doi:10.1029/2003JD003906, 2003.

Chen, R., Wood, R., Li, Z., Ferraro, R., and Chang, F.-L.: Studying the vertical variation of cloud droplet effective radius using ship and space-borne remote sensing data, J. Geophys. Res., 113, D00A02, doi:10.1029/2007JD009596, 2008.

Hansen, J. E. and Travis, T. D.: Light scattering in planetary atmosphere, Space Sci. Rev., 16, 527–610, 1974.

King, M.: Determination of the scaled optical thickness of clouds from reflected solar radiation measurements, J. Atmos. Sci, 44.13, 1734–1751, 1987.
Lebsock, M. D., Stephens, G. L., and Kummerow, C.: Multisensor satellite observations of aerosol effects on warm clouds, J. Geophys. Res., 113, D15205, doi:10.1029/2008JD009876, 2008.
Leon, D. C., Wang, Z., and Liu, D.: Climatology of drizzle in marine boundary layer clouds based on 1 year of data from CloudSat and CALIPSO, J. Geophys. Res., 113, DOOA14, doi:10.1029/2008JD009835, 2008.
Loeb, N. G., Varnai, T., and Winker, D. M.: Influence of subpixelscale cloud-top structure of reflectances from overcast stratiform cloud layers, J. Atmos. Sci., 55, 2960–2973, 1998.
Marshak, A., Platnick, S. E., Varnai, T., Wen, G., and Cahalan, R. F.: Impact of 3D radiative effects on satellite retrievals of cloud droplet sizes, J. Geophys. Res., 111, DO9207, doi:10.1029/2005JD006686, 2006.
Mayer, B.: Radiative transfer in the cloudy atmosphere, European Physical Journal Conferences, 1, 75–99, 2009.
Mayer, B. and Kylling, A.: Technical note: The libRadtran software package for radiative transfer calculations – description and examples of use, Atmos. Chem. Phys., 5, 1855–1877, 2005, http://www.atmos-chem-phys.net/5/1855/2005/.
Menzel, W. P., Frey, R., Zhang, H., Wylie, D., Moeller, C., Holz, R., Maddux, B., Baum, B. A., Strabala, K., and Gumley, L.: MODIS global cloud-top pressure and amount estimation: algorithm description and results, J. Appl. Meteorol. Clim., 47, 1175–1198, 2008.
Minnis, P., Arduini, R. F., Young, D. F., Ayers, J. K., Albracht, B. A., Sharon, T., and Stevens, B.: An examination of the impact of drizzle drops on satellite retrieved effective particle sizes, in: Proceedings of the 14th International Conference on Clouds and Precipitation, Bologna, Italy, July 2004.
Nakajima, T. and King, K. D.: Determination of the optical thickness and effective particle radius of clouds from reflected solar radiation measurements, Part 1: Theory, J. Atmos. Sci. 47, 1878–1893, 1990.
Platnick, S.: Vertical photon transport in cloud remote sensing problems, J. Geophys. Res., 105(D18), 22919–22935, 2000.
Platnick, S., Li, J. Y., King, M. D., Gerber, H., and Hobbs, P. V.: A solar reflectance method for retrieving the optical thickness and droplet size of liquid water clouds over snow and ice surfaces, J. Geophys. Res., 106(D14), 15185–15199, 2001.

Platnick, S., King, M. D., Ackerman, S. A., Menzel, W. P., Baum, B. A., Riedi, J. C., and Frey, R. A.: The MODIS cloud products: Algorithms and examples from Terra, IEEE T. Geosci. Remote, 41(2), 459–473, 2003.

Stevens, B., Vali, G., Comstock, K., Wood, R., van Zanten, M. C., Austin, P. H., Bretherton, C. S., and Lenschow, d. H.: Pockets of open cells and drizzle in marine stratocumulus, B. Am. Meteor. Soc., 51–57, 2005.

Vant-Hull, B., Marshak, A., Remer, L., and Li, Z.: The effects of scattering angle and cumulus cloud geometry on satellite retrievals of cloud drop effective radius, IEEE T. Geosci. Remote, 45(4), 1039–1045, 2007.

Varnai, T. and Marshak, A.: Statistical analysis of the uncertainties in cloud optical depth retrievals caused by three-dimensional radiative effects, J. Atmos. Sci., 58, 1540–1548, 2001.

Varnai, T. and Marshak, A.: View angle dependence of cloud optical thickness retrieved by MODIS, J. Geophys. Res., 112, D06203, doi:10.1029/2005JD006912, 2007.

Wood, R., Comstock, K. K., Bretherton, C. S., Cornish, C., Tomlinson, J., Collins, D. R., and Fairall, C.: Open cellular structure in marine stratocumulus sheets, J. Geophys. Res., 113, D12207, doi:10.1029/2007JD009371, 2008.

Zinner, T. and Mayer, B.: Remote sensing of stratocumulus clouds: uncertainties and biases due to inhomogeneity, J. Geophys. Res., 111, D14209, doi:10.1029/2005JD006955, 2006.

ACPD

10, 1221–1259, 2010

Drizzle and 3-D structure impact on effective size retrievals

T. Zinner et al.

ACPD
10, 1221–1259, 2010

Drizzle and 3-D structure impact on effective size retrievals

T. Zinner et al.

Table 1. Overview LES simulations.

LES case	size bins	size range	domain grid	Δx	Δz	droplet density	optical thickness	rain rate
Sc 2 p.m.	25	1–256 µm	64×64×64	52.5 m	stretched grid	30 cm^{-3}	7.8 (mean)	0.02 mm/h
Sc 6 p.m.							9.4 (mean)	0.05 mm/h
Cu	25	1–1100 µm	128×128×100	100 m	40 m	~50 cm^{-3}	up to 85	>1 mm/h

ACPD
10, 1221–1259, 2010

Drizzle and 3-D structure impact on effective size retrievals

T. Zinner et al.

Table 2. Average values over two analyzed stratocumulus scenes of true and retrieved values of effective radius and cloud optical thickness.

domain average	"true" r_{eff} [µm]	r_{eff} [µm] 0.86/**1.6**	r_{eff} [µm] 0.86/**2.1**	r_{eff} [µm] 0.86/**3.7**	true COT	COT retr.
1-D nodriz	16.16	13.83	16.15	16.49	8.46	9.38
1-D driz	16.44	14.11	16.42	16.58	8.75	9.68
3-D nodriz	16.16	13.67	16.28	16.65	8.46	9.26
3-D driz	16.44	13.95	16.57	16.75	8.75	9.55

Table 3. Standard deviation over two analyzed stratocumulus scenes of true and retrieved values of effective radius and cloud optical thickness.

standard deviation	"true" r_{eff} [µm]	r_{eff} [µm] 0.86/**1.6**	r_{eff} [µm] 0.86/**2.1**	r_{eff} [µm] 0.86/**3.7**	true COT	COT retr.
1-D nodriz	0.68	3.86	1.01	0.55	2.98	3.35
1-D driz	0.75	3.97	1.04	0.58	3.10	3.48
3-D nodriz	0.68	4.13	1.87	0.98	2.98	3.33
3-D driz	0.75	4.27	1.98	1.01	3.10	3.44

ACPD

10, 1221–1259, 2010

Table 4. Domain average values for the cumulus scene of true and retrieved values of effective radius and cloud optical thickness.

domain average	"true" r_{eff} [µm]	r_{eff} [µm] 0.86/**1.6**	r_{eff} [µm] 0.86/**2.1**	r_{eff} [µm] 0.86/**3.7**	true COT	COT retr.
1-D nodriz	19.87	11.02	14.71	21.27	2.19	1.71
1-D driz	58.42	10.23	14.58	22.14	2.26	1.75
3-D nodriz	19.87	7.41	11.72	21.28	2.19	1.06
3-D driz	58.42	7.73	11.65	21.93	2.26	1.09

ACPD
10, 1221–1259, 2010

Table 5. Standard deviation for the cumulus scene of true and retrieved values of effective radius and cloud optical thickness.

standard deviation	"true" r_{eff} [µm]	r_{eff} [µm] 0.86/**1.6**	r_{eff} [µm] 0.86/**2.1**	r_{eff} [µm] 0.86/**3.7**	true COT	COT retr.
1-D nodriz	9.00	9.20	9.91	6.91	9.33	13.27
1-D driz	48.76	8.75	9.70	7.47	9.32	13.45
3-D nodriz	9.00	6.98	9.03	8.47	9.33	6.46
3-D driz	48.76	7.32	9.38	8.60	9.32	6.56

ACPD

10, 1221–1259, 2010

Title Page
Abstract Introduction
Conclusions References
Tables Figures
◀I ▶I
◀ ▶
Back Close
Full Screen / Esc
Printer-friendly Version
Interactive Discussion

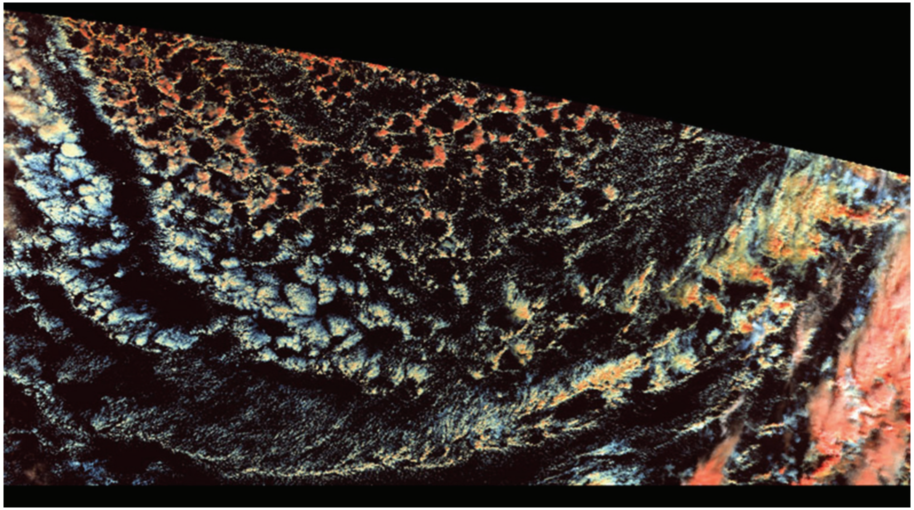

Fig. 1. False color composite (R, G, B=0.65, 1.6, 2.1 µm) of a stratocumulus scene over the northern subtropical Atlantic, 21 November 2004, 14:30 UTC, 1 km MODIS Terra data.

ACPD
10, 1221–1259, 2010

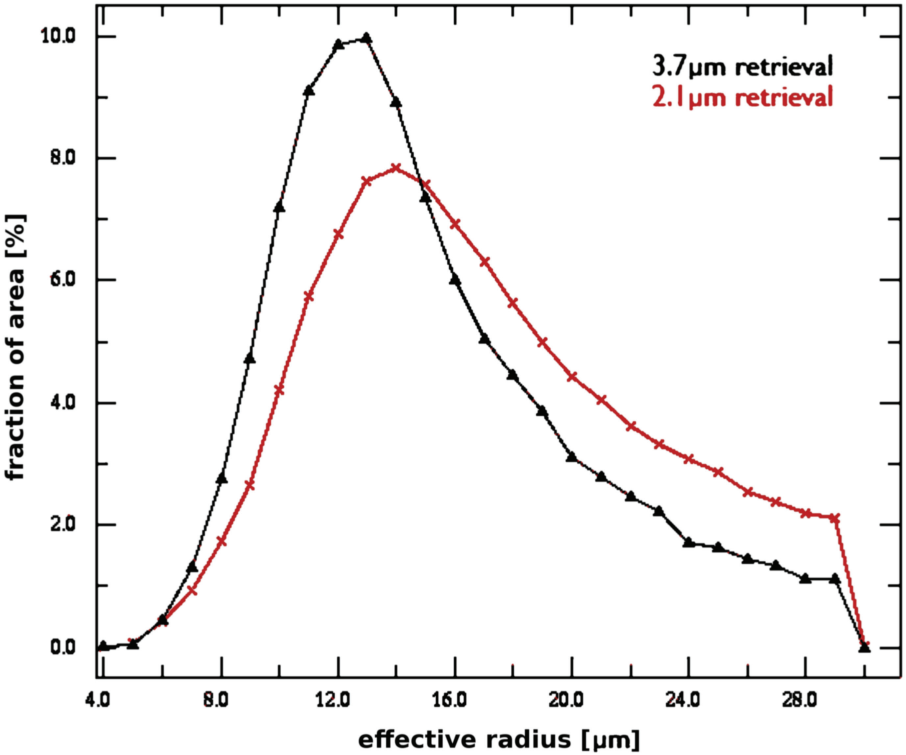

Fig. 2. Histogram of two MOD06 effective radius retrievals for the area of open cells in the upper left part of Fig. 1.

ACPD
10, 1221–1259, 2010

ACPD

10, 1221–1259, 2010

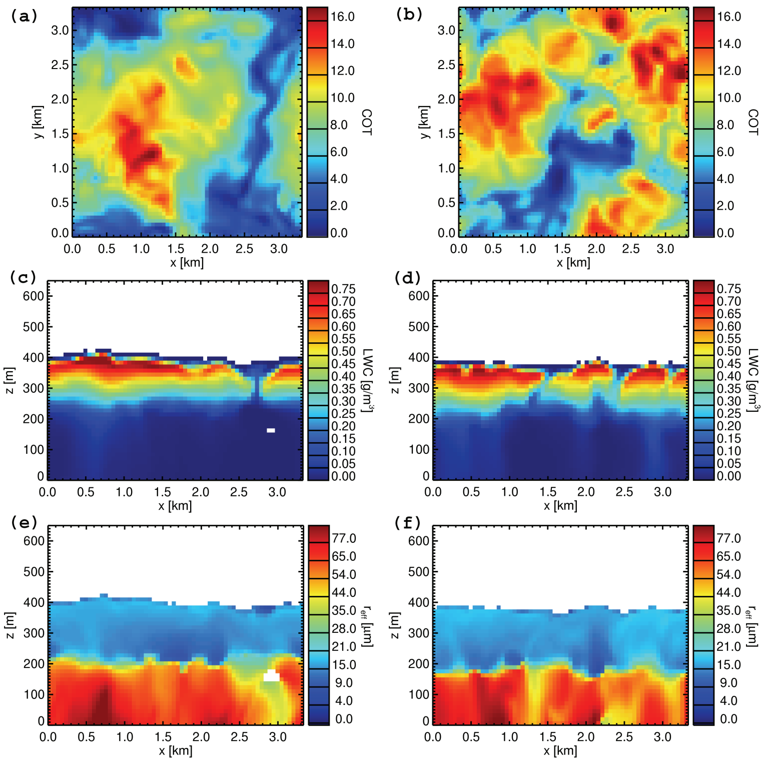

Fig. 3. Cloud data from large eddy simulations of marine stratocumulus deck, 64×64×64 boxes, 52.5×52.5 m horizontal resolution, vertical grid spacing varies between 6 and 100 m: (left) 2 p.m. local time and (right) 6 p.m. local time. Cloud optical thickness (COT), domain mean is 7.8 for 2 p.m. **(a)** and 9.4 for 6 p.m. **(b)**, liquid water content (LWC, **c, d**), r_{eff} **(e, f)**. Drizzle shows up as low LWC (<0.05 g/m^3) below ~200 m height associated with large effective radius values (>35 µm). The x-z vertical slices are taken at the y=1680 m. White areas have LWC<0.0001 g/m^3.

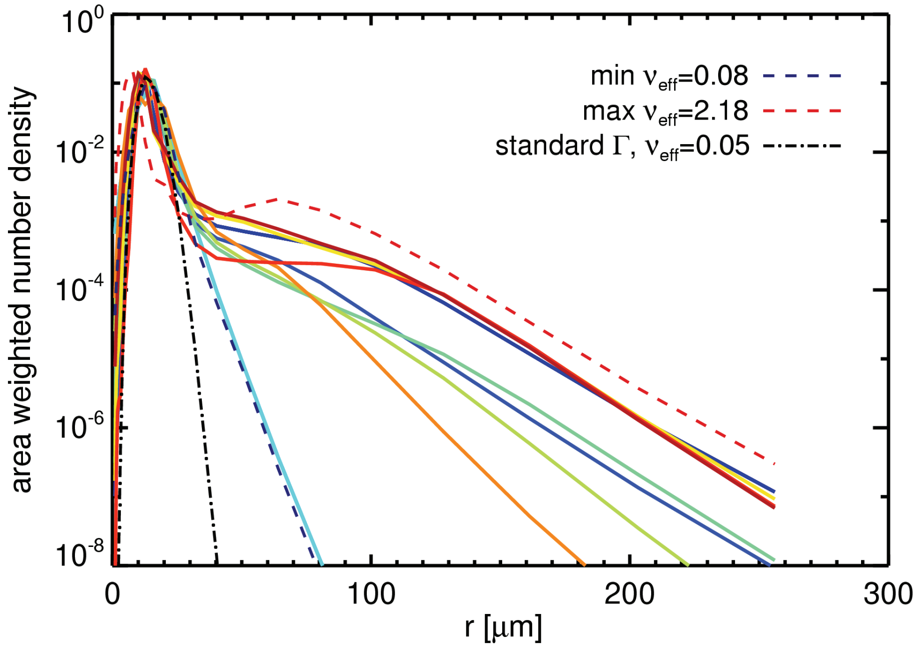

Fig. 4. Sample of 10 drop size distributions from the LES cloud model. All selected distributions have an effective radius of 15 µm (solid lines). The classical narrow Gamma distribution (ν_{eff}=0.05) is marked by the black dot-dashed line. 2% of all LES distributions are narrower than the one marked by the blue broken line (labeled "min", which is close to another typical standard value ν_{eff}=0.1) and 2% are wider than the one marked by the red broken line ("max").

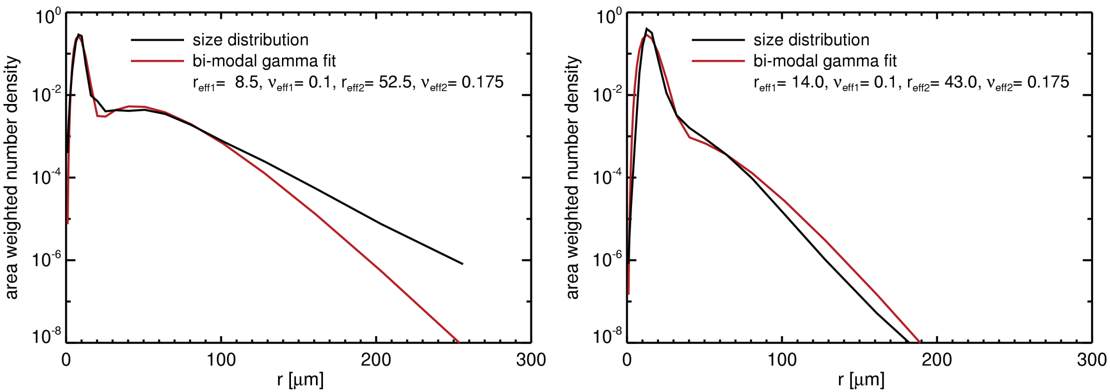

Fig. 5. Examples of bimodal Gamma function fit for two examples with original r_{eff}=15 µm from LES cloud data. Shown are the fit parameters for the two Gamma functions used.

ACPD
10, 1221–1259, 2010

Title Page
Abstract | Introduction
Conclusions | References
Tables | Figures
◀| |▶
◀ ▶
Back | Close
Full Screen / Esc
Printer-friendly Version
Interactive Discussion

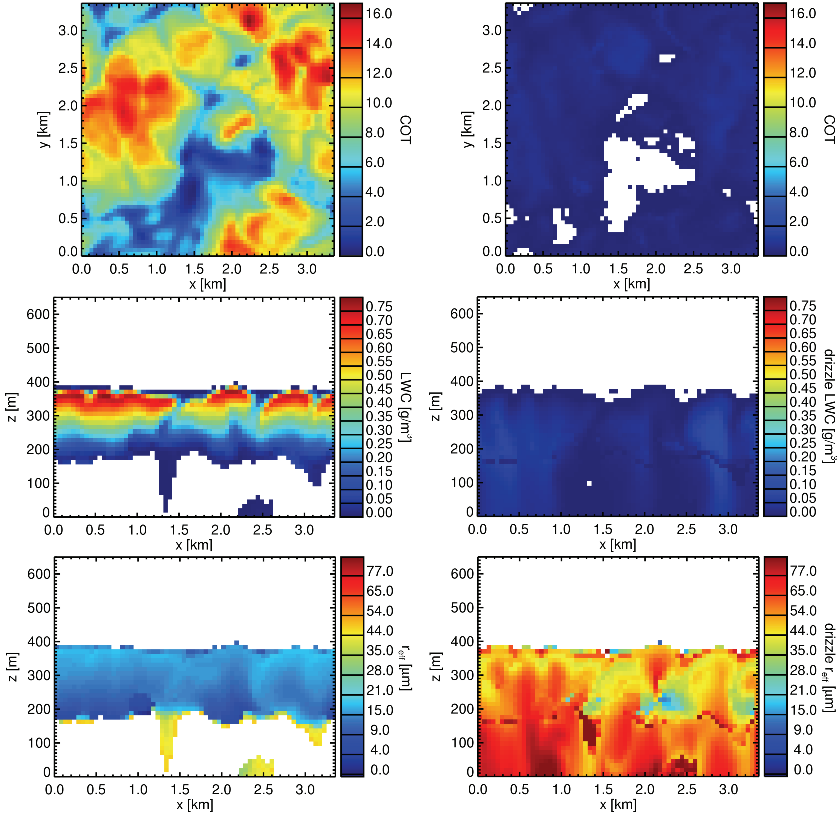

Fig. 6. Separation of drizzle and cloud modes (compare to Fig. 3 right column): (Left column) cloud droplet mode, (right column) drizzle drop mode. The mean optical thickness of the cloud droplet mode is 9.1, and the mean optical thickness of the drizzle mode is 0.4. White areas have LWC<0.0001 g/m^3.

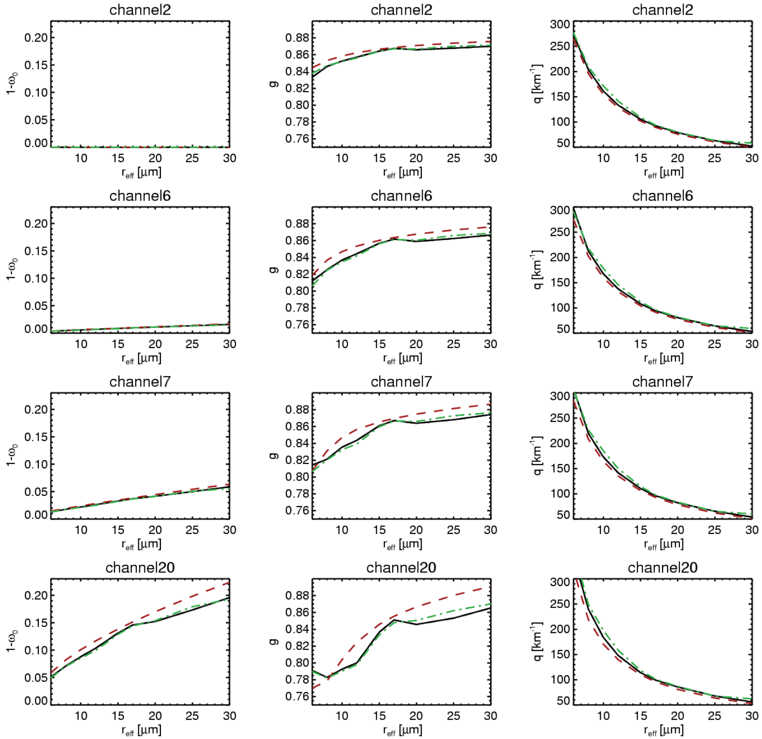

Fig. 7. Examples of Mie properties for MODIS channels 2 (0.8 μm), 6 (1.6 μm), 7 (2.1 μm), and 20 (3.7 μm). Values are averaged over 50 sample size distributions from the LES cloud data for each effective radius. Shown are the single scattering albedo ($1-\omega_0$, left), the asymmetry parameter (center), and the extinction per unit mass (per 1 g/m^3, right) calculated for the full given size distribution (black lines), for a standard narrow Gamma distribution (red dashed lines, $\nu_{\rm eff}$=0.1), and for the bimodal Gamma fit described above (green dot-dashed lines).

ACPD
10, 1221–1259, 2010

Drizzle and 3-D structure impact on effective size retrievals

T. Zinner et al.

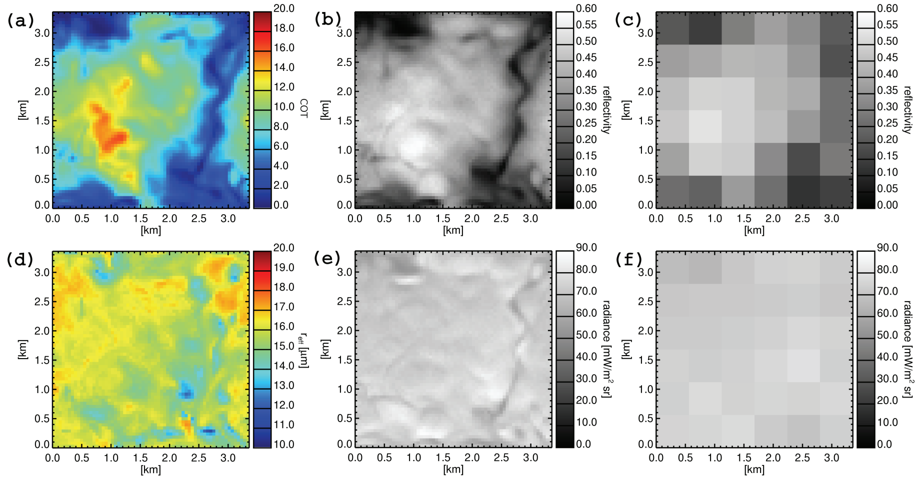

Fig. 8. Examples of simulated satellite observations for the LES stratocumulus scene at 2 p.m. (cf. Fig. 3). Shown is the optical thickness **(a)**, the particle effective radius near cloud top (see text for details, **d**), the 3-D simulated reflectance in MODIS channels 2 **(b, c)** and 20 **(e, f)** at 50 m and 500 m resolution ("MODIS" resolution). The solar zenith angle is 45° (sun from the "south"), the viewing zenith angle 0° (nadir).

ACPD

10, 1221–1259, 2010

Drizzle and 3-D structure impact on effective size retrievals

T. Zinner et al.

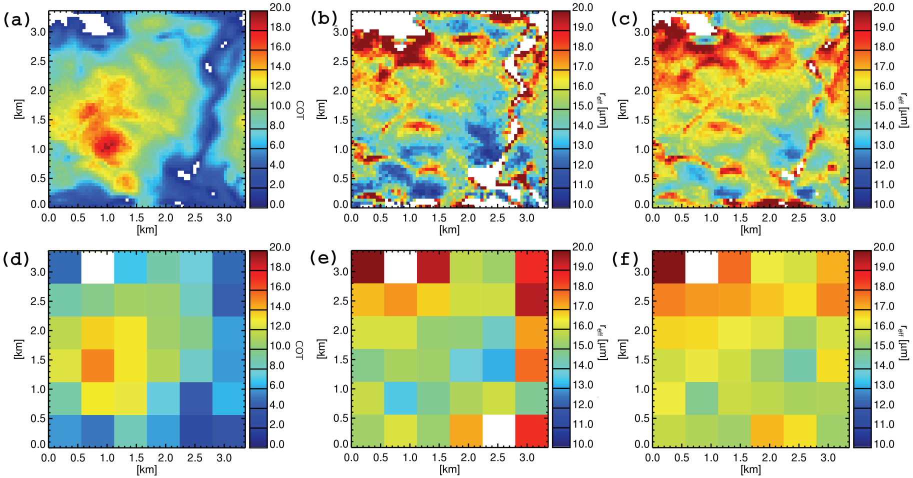

Fig. 9. MOD06 retrieval results for the 3-D simulated stratocumulus images (Fig. 8). Retrieved optical thickness on 50 m **(a)** and 500 m **(d)**, effective radius from 0.86/2.1 µm **(b, e)**, and from 0.86/3.7 µm **(c, f)**. For white areas no retrieval is found.

ACPD
10, 1221–1259, 2010

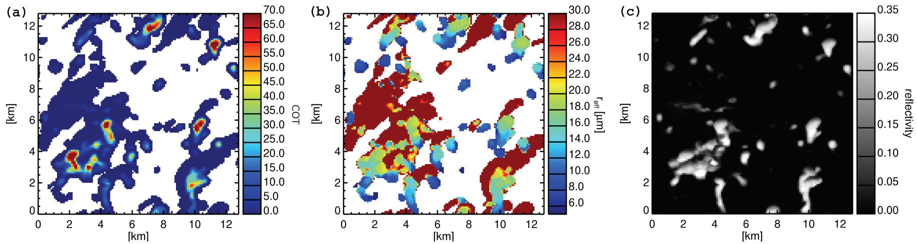

Fig. 10. Cumulus field – optical thickness **(a)**, cloud top layer effective radius **(b)**, simulated reflectivity in channel 7 (2.1 µm). The horizontal resolution is 100 m. Maximum values are cut off for reasons of presentation; white areas in **(a)** and **(b)** show COT=0.

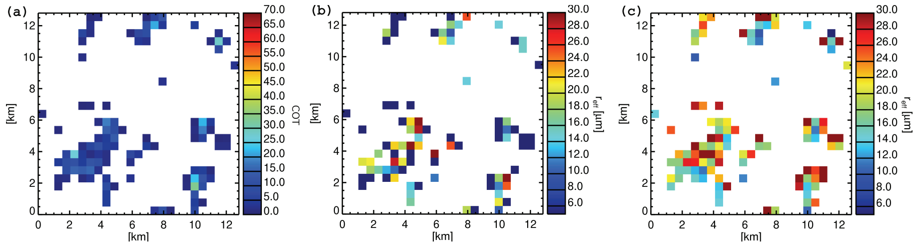

Fig. 11. MOD06 retrieval for 3-D cumulus simulations (500 m resolution) of optical thickness **(a)**, effective radius from 0.86/2.1 µm **(b)**, effective radius from 0.86/3.7 µm **(c)**. For white areas no retrieval is found.

ACPD
10, 1221–1259, 2010

Title Page
Abstract | Introduction
Conclusions | References
Tables | Figures
◀| |▶
◀ ▶
Back | Close
Full Screen / Esc
Printer-friendly Version
Interactive Discussion